Performance of the fuel model FFRS

Misfeldt, I.

Publication date:
1977

Document Version
Publisher's PDF, also known as Version of record

Citation (APA):
Misfeldt, I. (1977). *Performance of the fuel model FFRS*. Risø National Laboratory. Risø-M No. 1928

A. E. K. Risø

Risø - M - 1928

Risø - M - 1928

Title and author(s)

Performance of the Fuel Model FFPS

by

Ib Misfeldt

Date 28 March 1977

Department or group

Department of Reactor Technology

Group's own registration number(s)

RT-10-14

IM/rj

11 pages + tables + 8 illustrations

Abstract

FFRS, a computer code for simulation of in-pile fuel rod performance, was developed for use in reliability predictions for nuclear fuel. Since this application involves numerous fuel simulations, the model is sufficiently simple to allow for fast computer calculation, but still detailed enough for realistic simulation.

The performance of the model was examined by analyzing several cases, including the four EPRI Benchmark cases (described in CENFD-218) as well as experiments from the Danish irradiation programme.

It was demonstrated that the model is based on sound principles, representing the state of the art in fuel modelling. It is therefore a valuable tool giving reliable results a very small computer costs.

Copies to

Library 100
RT 12
I. Misfeldt 30

Available on request from: Risø Library, Research Establishment Risø, DK-4000 Roskilde, Denmark.
Risø Bibliotek, Forsøgsanlæg Risø, 4000 Roskilde
Telephone: (03) 35 51 01, ext. 334, telex: 43116.

Fi 25-204

ISBN 87 550-0454-7

CONTENTS

1. INTRODUCTION

The need for a fast fuel model was realized at the start of the Danish project on fuel reliability prediction. The model needed to be orders of magnitude faster (in computer time) than the existing Danish fuel performance code Hotcake[1], but not necessarily self-contained, since it could be adjusted by comparison with Hotcake. Correct response to reasonable changes in the design data, material properties and operational conditions was the desired capability of the model. Since the type of failure with which we are most concerned is pellet-clad interaction, modelling was concentrated on fuel-clad contact situations.

The approach chosen was very successful compared to other fuel models, therefore the model was completed as a self-contained fuel performance code, FFRS. After completion of the code, it was tested on several sample cases. The results are generally in as good agreement with experimental data as are the predictions by state-of-the art fuel models; the fuel-clad contact results seem especially successful.

2. SHORT DESCRIPTION OF FFPS

A slice (disc) of the fuel rod is treated in the model. For fission gas release and internal pressure, an approximation to the whole rod is used. The slice is divided into 5 regions: clad, gap, fuel rigid zone, bridge and fuel plastic zone. The model for the different regions is:

Clad

Axisymmetrical, hollow, thin cylinder with a pressure difference between the outside and the inside, and a superimposed axisymmetrical contact pressure on the inside. Elastic, plastic, thermal and creep strains are considered. Primary creep and plastic strain are strain hardening, the strength coefficients are fluence dependent.

Gap

The gap forms the boundary between fuel and clad. The heat transfer through the gap is modelled according to Ross and Stoute[2].

Fuel, all regions

The temperature distribution is calculated on the basis of heat generation with flux depression and heat transfer[3]. Simple models for densification (burnup dependent), swelling (temperature dependent) and fission gas release (temperature dependent) are included.

Fuel, rigid

The rigid zone is assumed to be cracked, the thermal expansion is calculated as that of a rigid bar. No creep, plastic or elastic deformation occur.

Fuel, plastic

The material in the plastic zone is allowed to expand freely and is assumed to be stress-free, except for hydrostatic pressure.

Bridge

A rigid annulus, the bridge, forms the boundary between the rigid and the plastic fuel zones. The position of the bridge, together with the temperature distribution in the fuel, determines the thermal expansion of the cracked pellet.

During steady power conditions the movements of the bridge are determined by the creep rate at the bridging annulus, and the total crack opening angle, see fig. 1.

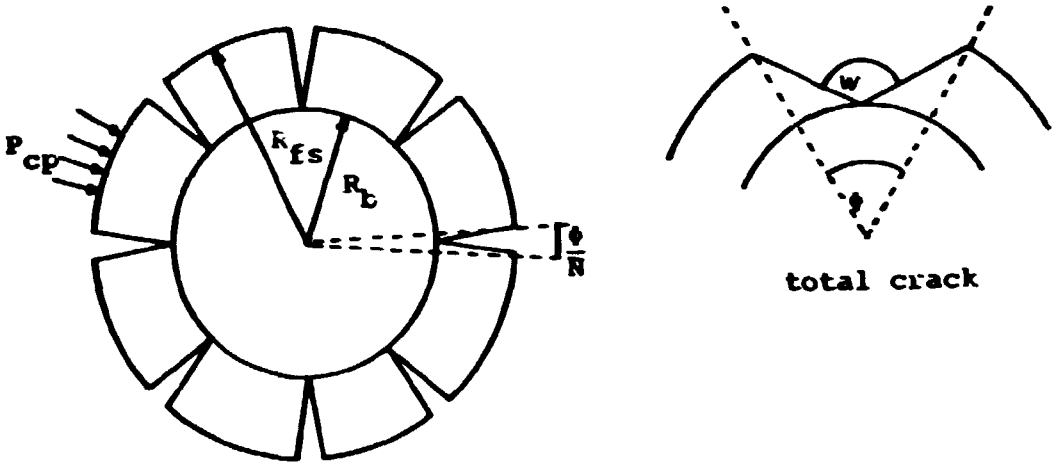

Fig. 1. Cracked pellet

The stress at the bridge is:

$$\sigma_b = P_{cp} * R_{fs}/R_b$$

where P_{cp} is the contact pressure, R_{fs} the fuel surface radius and R_b the bridge radius. The UO_2 creep, ε, at the bridge is found from the bridge temperature and σ_b by the UO_2 creep equation. The area which the material from P_b to $P_b + dP$ will occupy as a result of creep is:

$$A_{cr} = \varepsilon * dP * 2\pi * P_b;$$

the crack area between P_b and $P_b + dP$ may be approximated by:

$$A_{crk} = \pi * (dR)^2 * w/2\pi.$$

Equating these areas yields the creep of the bridge:

$$dR = \varepsilon * 4\pi/w.$$

Power ramps are divided into "small" ramps. In each "small" ramp the bridge is moved a fraction of the pellet radius towards the centre and then allowed to creep back as far as the creep rate and the time allow. Hence the bridge position is fixed by a balance between ramp rate and creep rate at the bridge.

Material properties

The material equations used in all the simulations are described in detail in[4].

3. CODE RESULTS ON THE FOUR EPRI CASES

The four EPRI cases[5] were chosen to demonstrate the performance of the model. They offer a variety of experimental data together with the predictions of several state-of-the-art fuel models. Since FFRS was primarily developed for pellet-clad interaction (PCI) predictions, cases A and B (small gap and stable fuel) are the most relevant, but calculations are included of cases C and D (large gap, unstable fuel) for completeness.

A description of the experiments including the design data is found in[5]; the results from FFRS are drawn on the figures from[5]. The curves presented are primarily those including some experimental results. As an illustration of the calculated stresses, tangential stress and contact pressure are shown for case A. For the two unstable cases (cases C and D) the hot gap is also shown.

Case A, the HCD rod (figures 2 - 8)

Case A was calculated with and without the suggested densification of 1%. The results are in good agreement with the experimental data. The permanent strain is mainly the result of primary creep, which is very low in the standardized material equations as proposed in the EPRI study[5]. FFRS does not use this creep equation, and thus gives a better prediction.

Case B, CANDU rods (figures 9 - 14)

Case B was calculated with σ_y = 364 MP at 300°C (the EPRI value) and with σ_y = 290 MP at 300°C (normal BWR clad). Again, the creep calculated by FFRS agrees well with the experimental data. The calculated hoop stress and contact pressure are in good agreement with the other codes, except for the final ramp where a pronounced difference appears. This difference originates from the relaxation that takes place in the pellet during the steady power period and seems well modelled in FFRS. The maximum temperatures are in good agreement with the experimental values.

Case C, ELP-9 Rod (figures 15 - 17)

This case is rather special due to the unstable fuel, the low clad temperature and the low system pressure. Since FFPS does not predict contact, the case mainly demonstrates the swelling, fission gas release, gap conductance and densification models; as mentioned, they are quite primitive (as in most state-of-the-art fuel models). The overall results are in as good agreement with the experimental results as any of the other codes. The results are shown on figures 15 - 17.

Case D, PWR Rod (figures 18 - 21)

Also this case is very dependent on densification, fission gas release, gap conductance and swelling. FFPS shows a strong instability in the temperature calculation. A small change in the residual gas (helium) assumed in the fuel will change the temperatures after the ramp at ~ 10000 hours, giving either a large fission gas release or almost no fission gas release.

The calculated temperatures at 93 in are shown on fig. 18 for two different assumed contents of residual gas. The other results (figs. 19 - 21) are shown corresponding to the high fission gas release; this was obtained with a "small" amount of residual gas. If an amount of residual gas corresponding to the fill gas is assumed, the calculated gas release is only 1.5%

The total calculation time for the four cases (HCD Rod, X-260 Rod, ELP-9 Rod, and the PWR rod at 10 and 93 in) was 31 s on a B6700, corresponding to 0.5 s on the CDC-7600. The codes in the EPRI investigation used between 54 and 721 s for the four cases.

4. ANALYSIS OF TWO DANISH RAMP TESTS

To study the performance of FFRS under very rapid power changes, an analysis was made of two ramp tests[6] performed at Risø on BWR fuel pins.

The two pins were irradiated to approximately 20.000 MWD/tUO_2 in the Halden reactor (34 at and 240°C) during 2½ years at power. Fig. 22 shows the Halden bundle power. The pins were ramp-tested in the Danish test reactor DR 3 at normal power reactor conditions (70 at ~ 300°C). Figures 23 and 24 show the ramp power histories. Though they were almost equal in design and preirradiation history, the two pins failed at 470 W/cm and 720 W/cm, respectively.

Due to the special irradiation conditions in the Halden reactor, almost no creep-down of the clad occurred during the preirradiation. FFPS does not include any model for relocation of the fuel and the temperatures in the fuel were too low for any hot-swelling to occur; therefore FFRS does not predict contact until around 500 watt/cm in any of the two ramps. On figs. 25 to 28 the generalised stress and the hoop strain are shown. It is obvious from the figures that no failures are predicted. If the as-fabricated gap is sufficiently reduced for the pins to come very close to contact during the Halden irradiation (gap size reduced by 40%), the response is more reasonable, as seen on figures 25 - 28. This discrepancy between the experiment and the code prediction could perhaps be explained by the lack of modelling of fuel relocation, but it could also be a stochastic matter. The latter idea seems promising because of the large sensitivity to the as-fabricated gap and the contradiction between the two ramp tests.

Since FFRS calculates average stress and strain in the clad, the local stress and strain during a ramp is considerably

higher. Therefore care should be taken when utilizing failure data obtained under controlled stress conditions, such as total elongation in tensile tests or time-to-failure in stress corrosion tests.

5. CONCLUSION

The fuel model FFRS is presented. It is shown that, in spite of its simplicity, the model can very accurately model average pellet-clad interaction. Calculations on the four EPRI test cases show that a variety of designs and test conditions can be successfully simulated. The problems arising, specially in case D, are probably due to gap conductance. The model used for gap conductance[6] is the same as in HOTCAKE[1], where similar problems were observed. This gap conductance model is currently under revision and we hope to solve the problems.

The calculation times used by FFRS are two to three orders of magnitude lower than those of typical state-of-the-art fuel codes.

6. REFERENCES

1. N. Kjær-Pedersen, HOTCAKE/TR-A. One-Dimensional Fuel Performance Code with Ridging Capability. Paper to Enlarged HPG-Meeting, Marts 1977.

2. A.M. Ross and R.L. Stoute, Heat transfer Coefficient between UO_2 and Zircaloy-2. AECL-1552 (1972).

3. M.J.F. Notley, A.S. Bain and J.A.L. Robertson, The Longitudinal and Diametral Expansion of UO_2 Fuel Elements. AECL-2143 (1964).

4. I. Misfeldt, unpublished material.

5. M.G. Andrews, H.R. Freeburn and S.P. Pati, Light Water Reactor Fuel Rod Modeling Code Evaluation, Phase II Topical Report. CENPD-218 (1976).

6. Combustion Engineering report, Fuel Evaluation Model, CENPD-139-A (1974).

7. P. Knudsen, C. Bagger and N. Kjær-Pedersen, Analysis of Overpower Performance of High-Burn-up Pellet and Vipac UO_2-Zr Fuel Pins, ANS Int. Conf. on World Nuc. Power, Nov. 1976.

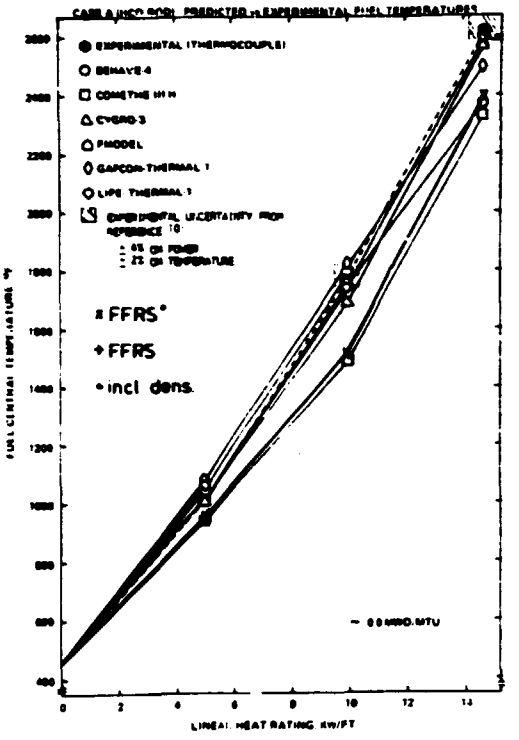

Fig. 2. CASE A Predicted vs. experimental fuel temperatures, BOL [*].

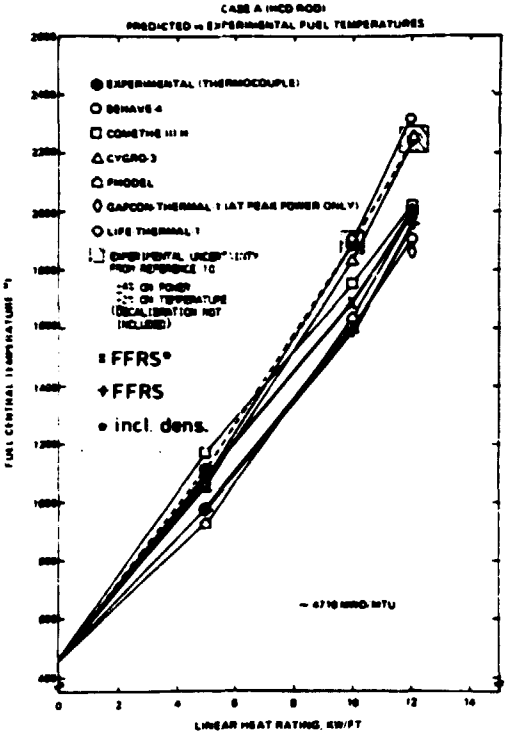

Fig. 3. CASE A. Predicted vs. experimental fuel temperatures [*].

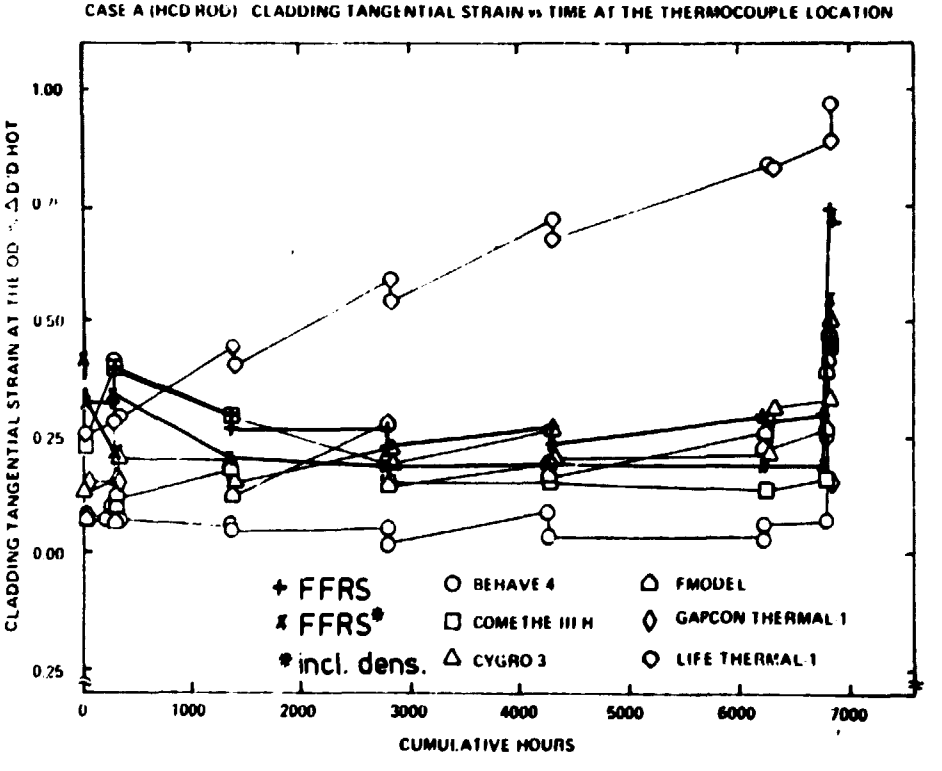

Fig. 4. CASE A. Cladding tangential strain vs. time[*].

[*] The results for FFRS are drawn on the figures from ref. 6.

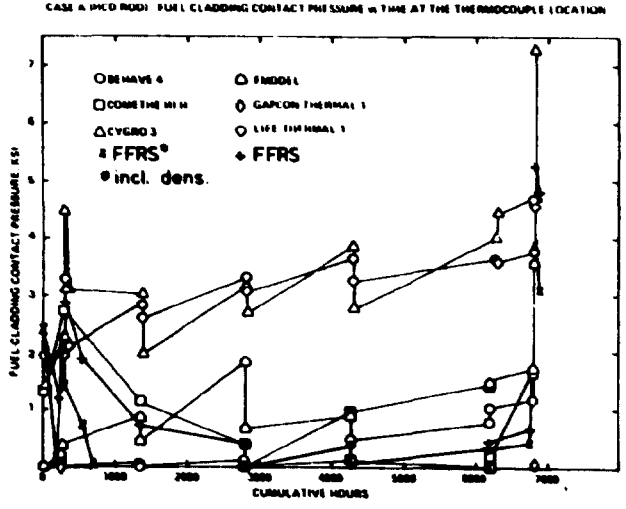

Fig. 5. CASE A. Fuel-clad contact pressure*

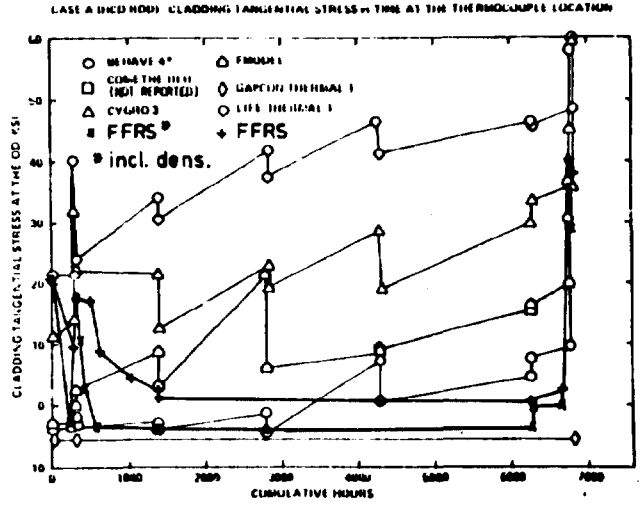

Fig. 6. CASE A. Clad tangential stress vs. time*.

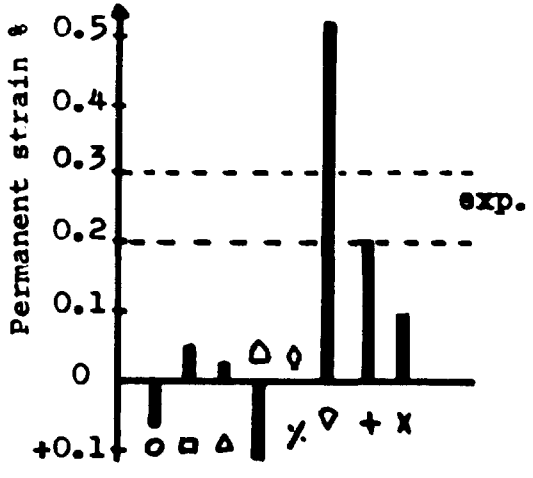

Fig. 7. CASE A. Permanent strain, EOL

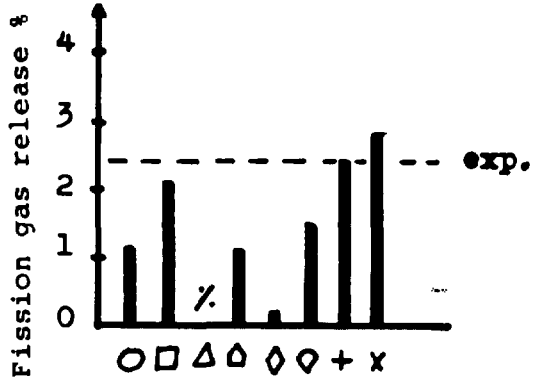

Fig. 8. CASE A. Fission gas release, EOL.

* The results for FFRS are drawn on the figures from ref. 6.

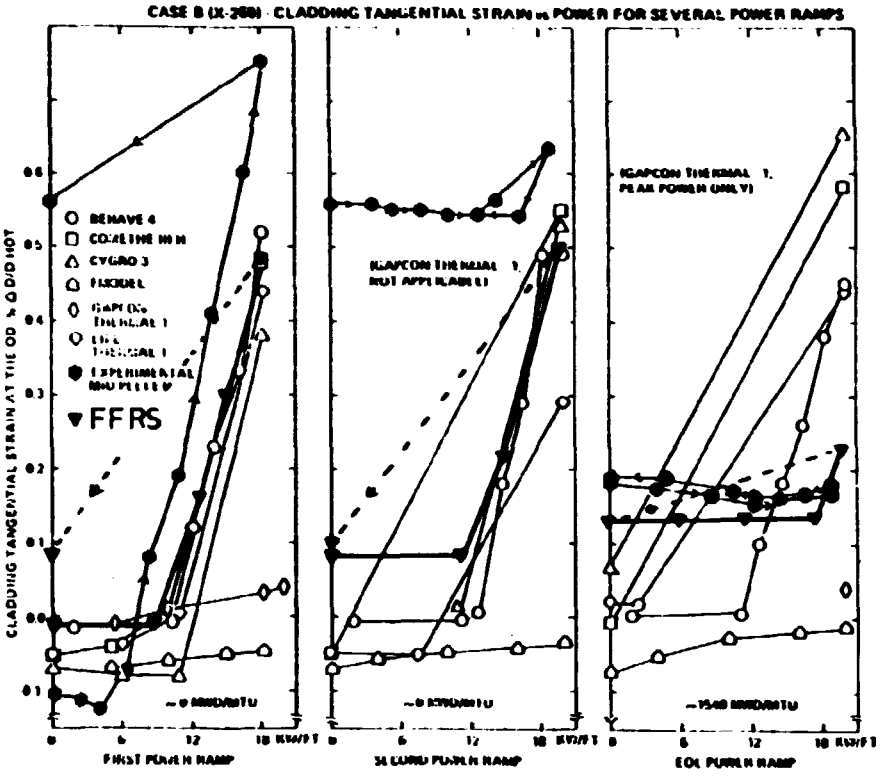

Fig. 9. CASE B (X-260). Cladding tangential strain vs. power*.

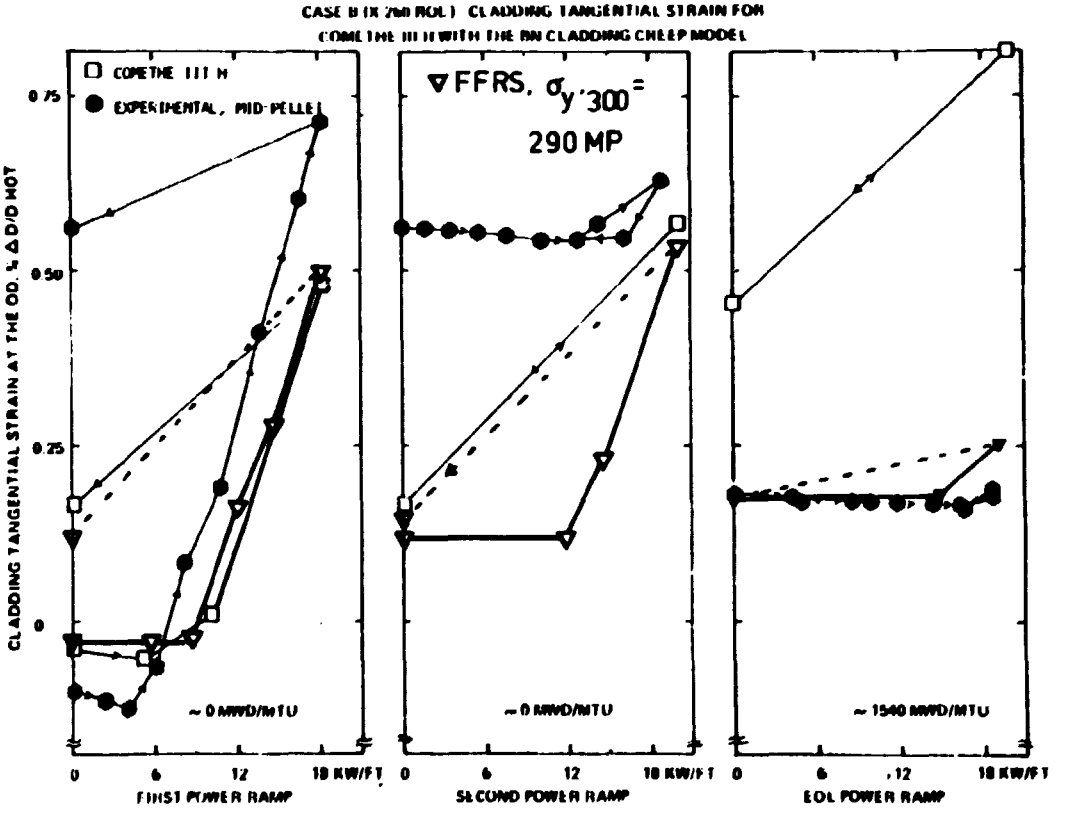

Fig. 10. CASE B (X-260). Cladding tangential strain vs. power, alternative creep models*.

* The results for FFRS are drawn on the figures from ref. 6.

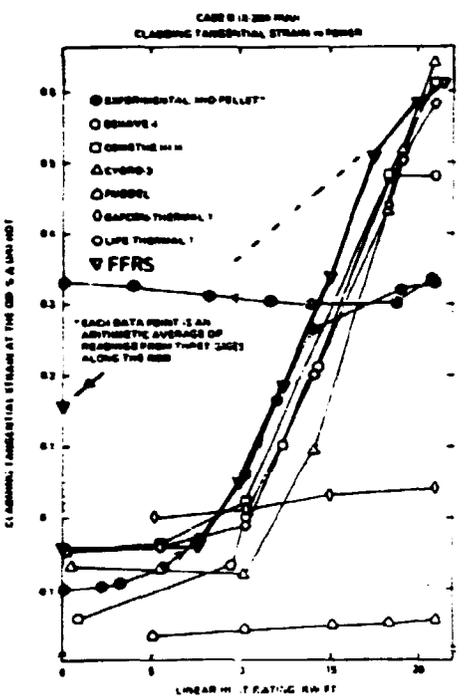

Fig. 11. CASE B (X-264). Cladding tangential strain vs. power*.

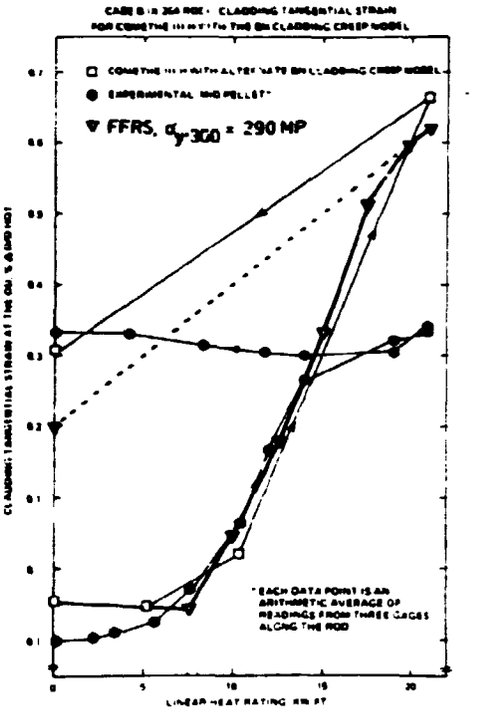

Fig. 12. CASE B (X-264). Cladding tangential strain vs. power, alternative creep models*.

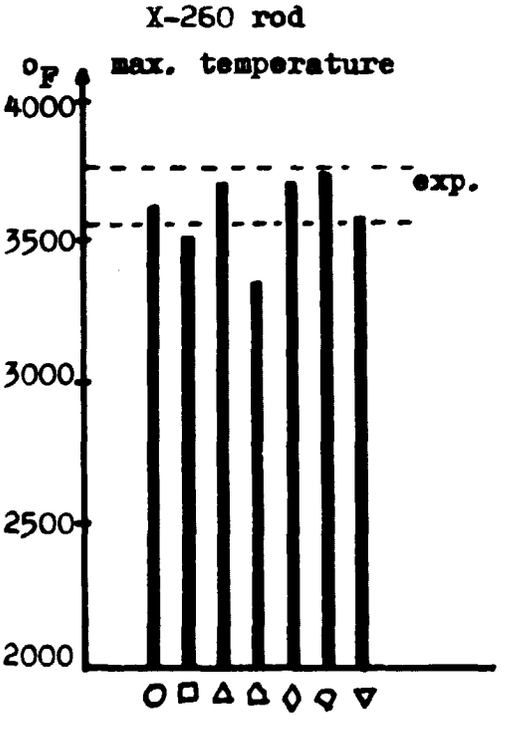

Fig. 13. CASE B (X-260). Maximum temperature

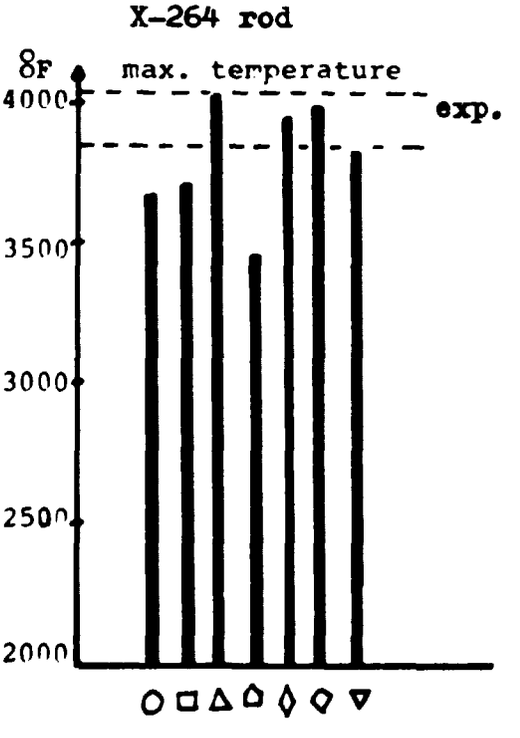

Fig. 14. CASE B (X-264). Maximum temperature

* The results for FFRS are drawn on the figures from ref. 6.

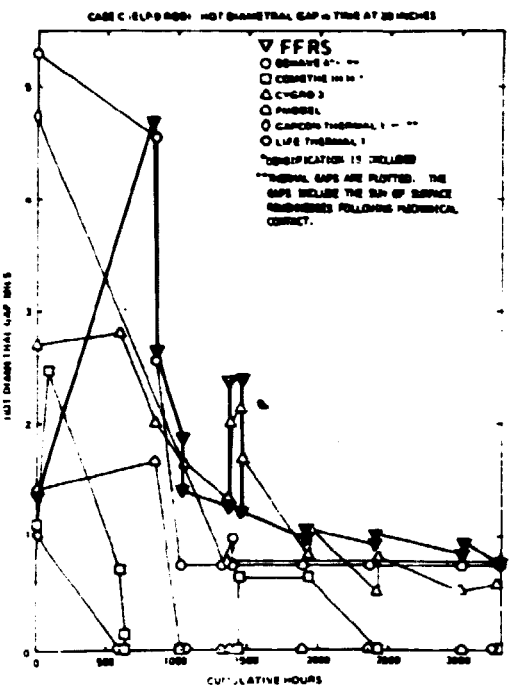

Fig. 15. CASE C. Hot diametral gap vs. time at 20 inches*.

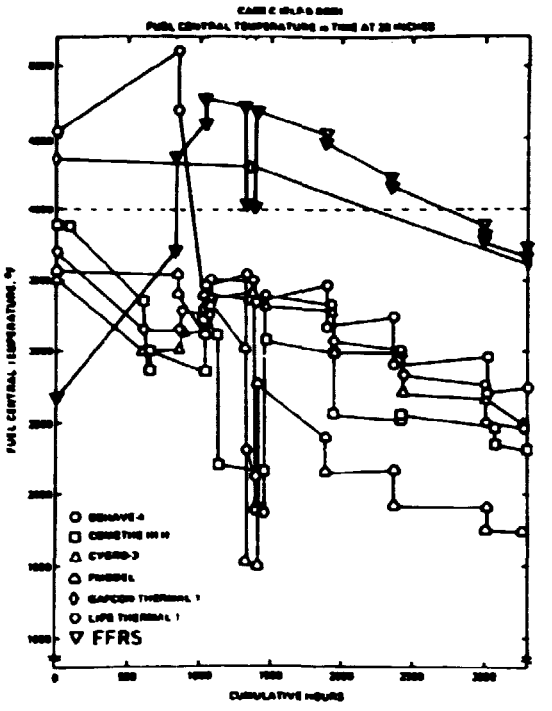

Fig. 16. CASE C. Fuel central temperature vs. time at 20 inches*.

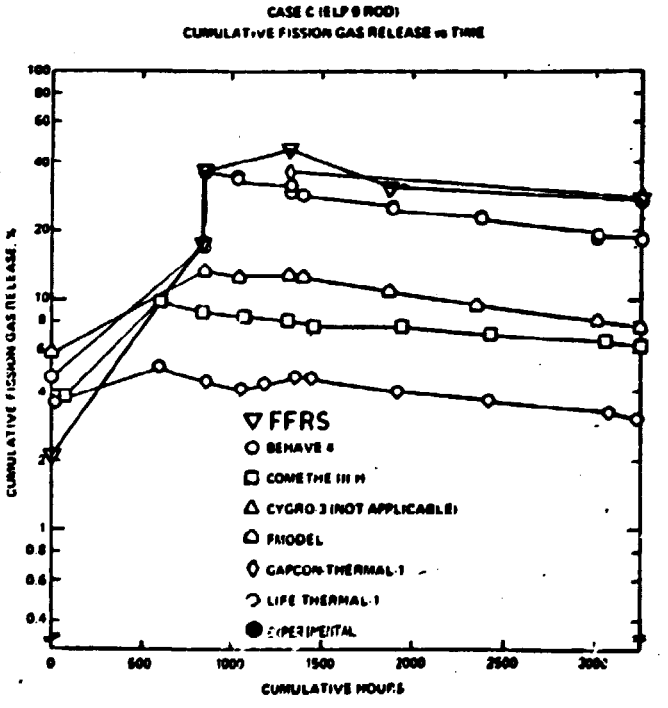

Fig. 17. CASE C. Cumulative fission gas release vs. time*

* The results for FFRS are drawn on the figures from ref. 6.

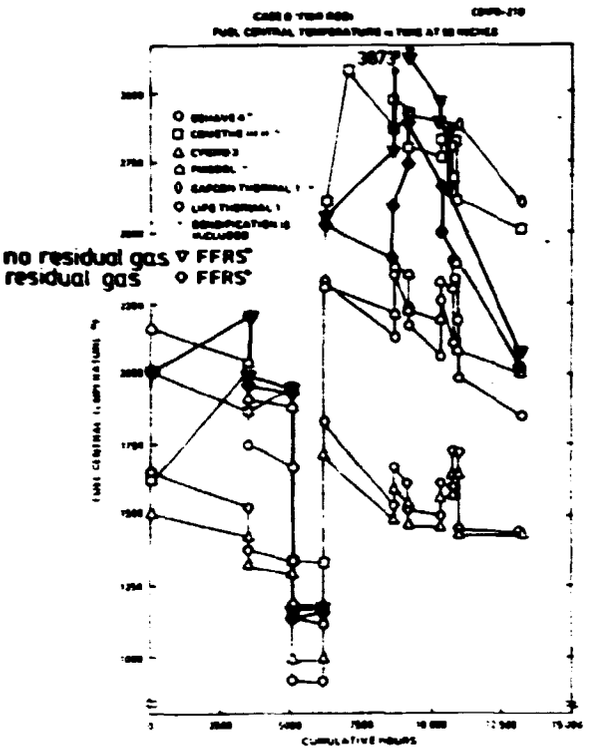

Fig. 18. CASE D. Fuel central temperature vs. time*.

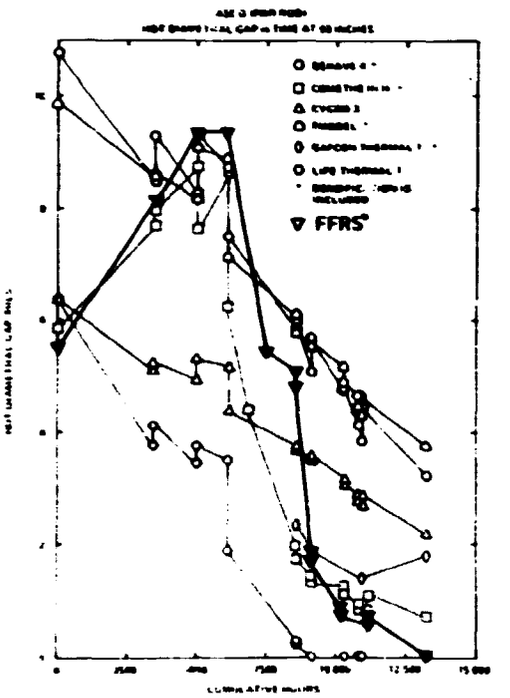

Fig. 20. CASE D. Hot diametral gap vs. time at 93 inches*.

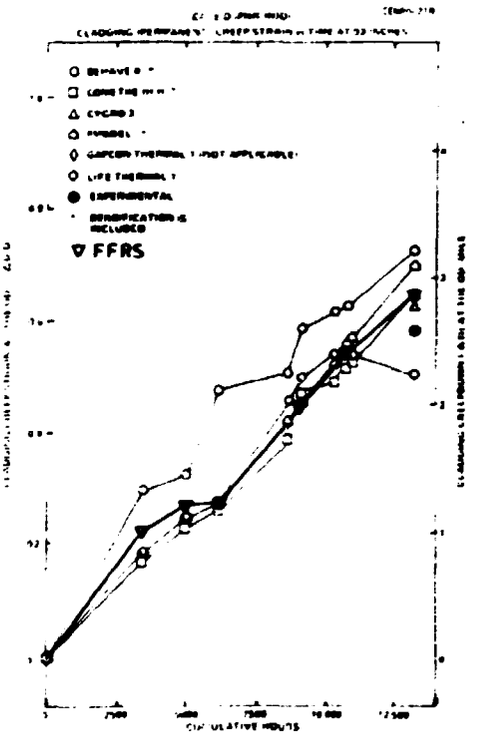

Fig. 19. CASE D. Cladding permanent strain vs. time at 93 inches*.

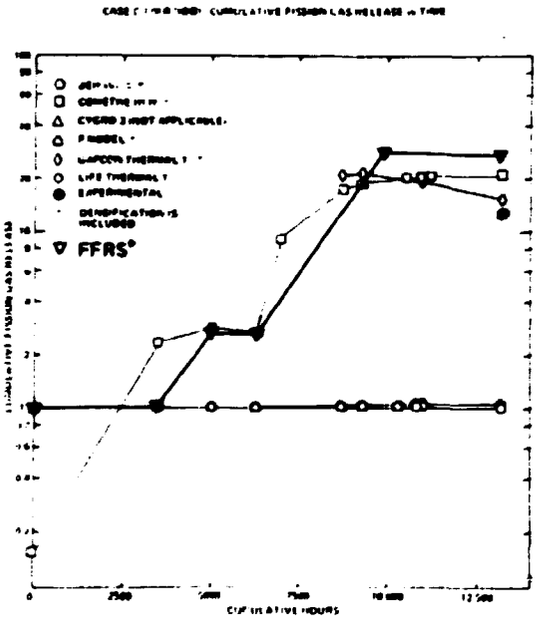

Fig. 21. CASE D. Fission gas release vs. time*.

* The results for FFRS are drawn on the figures from ref. 6.

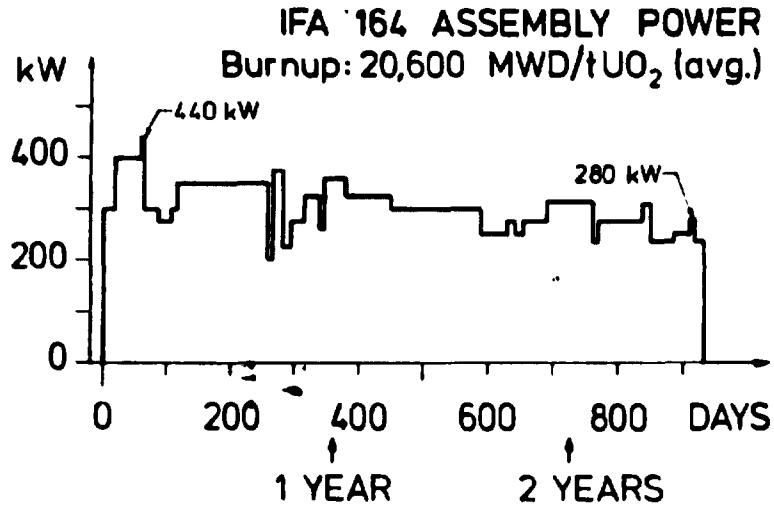

Fig. 22. Assembly power during the Halden irradiation.

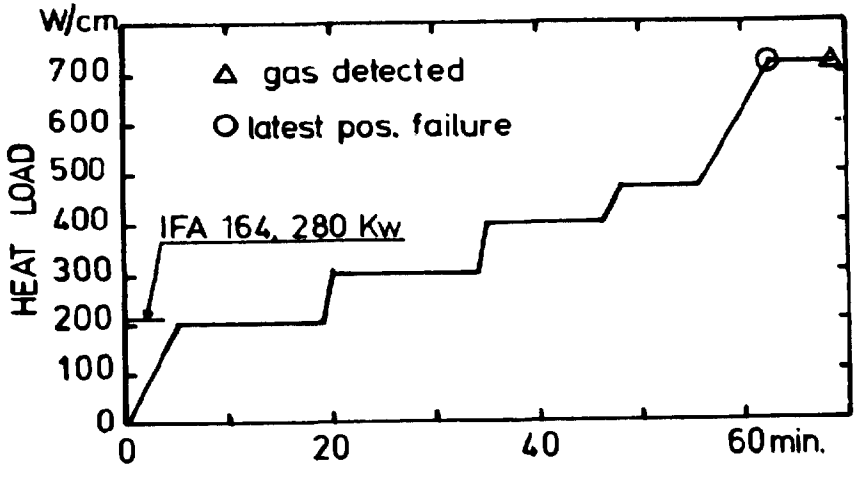

Fig. 23. Power ramp for PA21-3

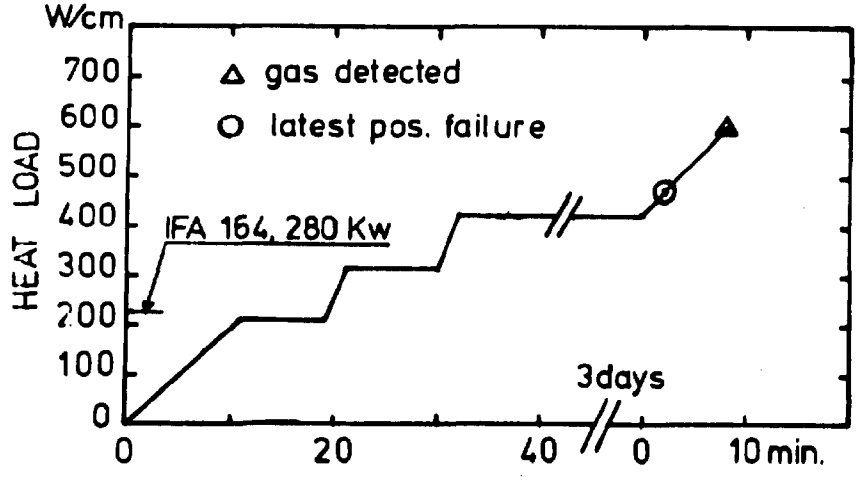

Fig. 24. Power ramp for PA24-2

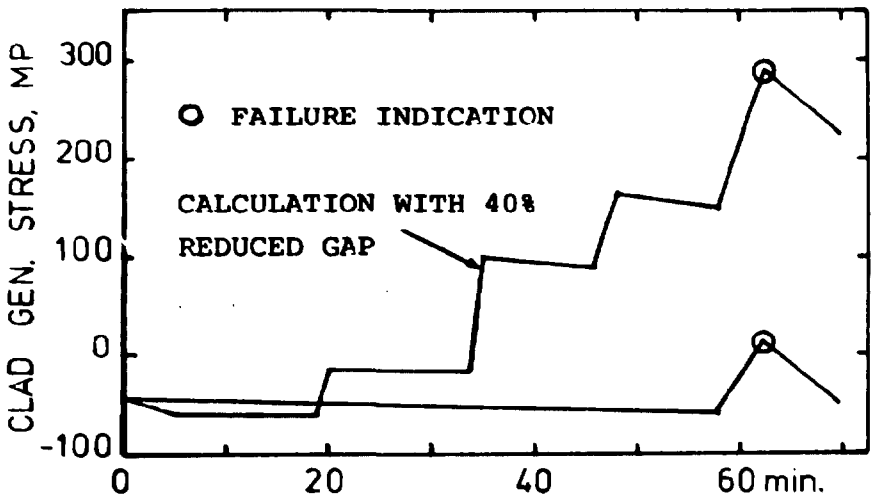

Fig. 25. Generalized clad stress of PA 21-3.

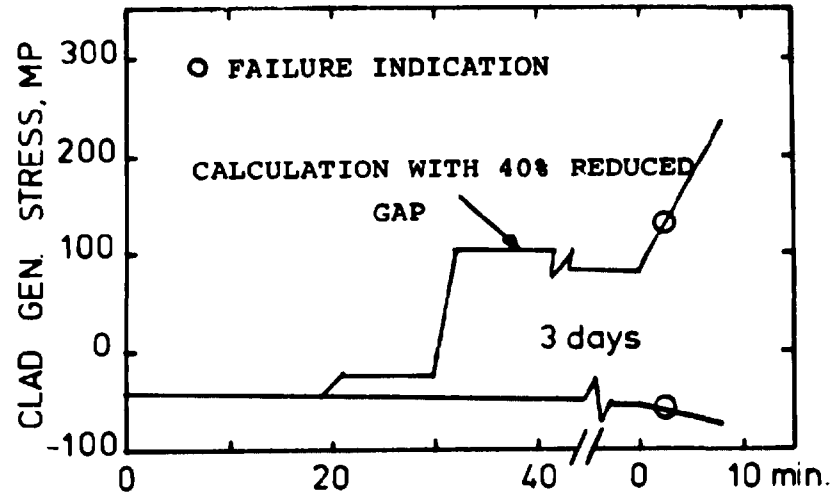

Fig. 26. Generalized clad stress of PA 24-2.

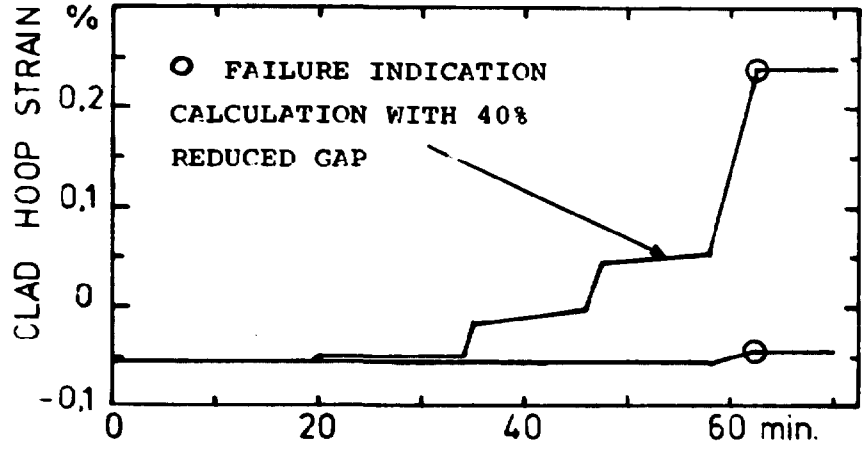

Fig. 27. Clad hoop strain of PA 21-3.

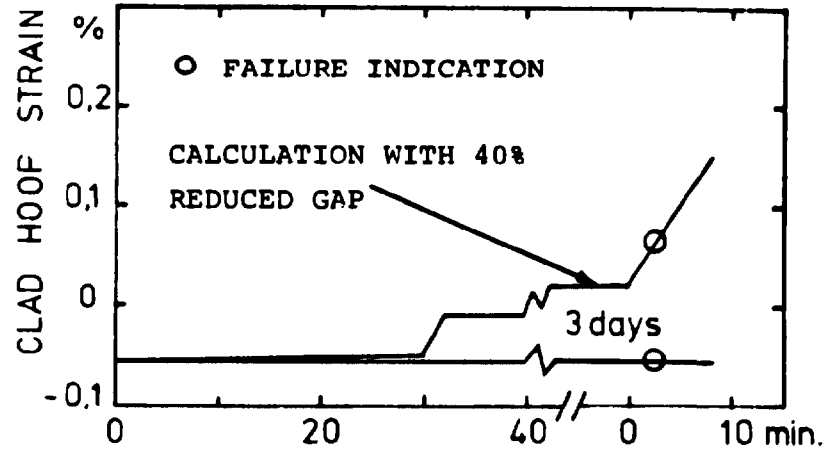

Fig. 28. Clad hoop strain of PA 24-2